UNIVERSITÉ PARIS DIDEROT (Paris 7)
SORBONNE PARIS CITÉ

LABORATOIRE
MATÉRIAUX ET PHÉNOMÈNES QUANTIQUES

M2 Quantum Devices

Benjamin WIRTSCHAFTER

Internship Report

Sympathetic cooling of $^{9}Be^{+}$ ion(s) in a $^{88}Sr^{+}$ crystal: a test for GBAR experiment.

M. Luca GUIDONI **Internship supervisor**

March to July 2017

Left blank on purpose

Acknowledgements

The work presented in this Master's report couldn't have been done without the help of a lot of people that I would like to acknowledge.

I would like to thank first the whole Trapped Ions team for welcoming me among them during these few months. More specifically I would like to warmly thank my internship supervisor Luca Guidoni, for the orientation he gave me, all his experience and scientific knowledge that he shared with me, and for re-reading this report. Many thanks to Jean Pierre Likforman for his enthusiasm - *I'm thinking about the first time we photoionized strontium with the new setup* - and all the things he taught me, particularly in the field of lasers, in which my knowledge and experience as I realize it now, were quite limited. My gratitude to Albane Douillet from the LKB, for the things she taught me and for answering to my interrogations. I would like to thank Samuel Guibal for the help that he provided and congratulate him again for his HDR. I would like to thank Vincent Tugayé for his help, and for sharing the experiment with me. I wish to all the team good luck for the following of the experiment and the future ones. From a few meter outside the lab, I would like to thank Sara Ducci for the great chance she gave me two years ago and for the help provided at the beginning of the year, for which I am very grateful.

Apart from work, I would like to thank Vale, my friends, and family, for their unconditional support and especially my parents for everything they have done for me.

Contents

Introduction:

Observations of the universe at large scales gave rise to fundamental questions during the last century. Those observations led to the introduction of the dark energy to explain the acceleration of the expansion of the universe, but also of the dark matter to explain the missing mass in the global dynamic of galaxies and other larger structures. These misknown theoretical objects combined with observation suggest that our understanding of gravitation - although never been disproven up to now(1) - might be incomplete. Also, in the *big bang theory*, antimatter is supposedly « created » in the same proportion than matter initially. However, this is not observed in the universe today. One can ask why this primordial symmetry did not prevail.

A recent european experiment called Gravitational Behavior of Anti-hydrogen at Rest (GBAR), aims to investigate that matter, by verifying the Einstein's principle of equivalence. This principle is one corner stone of general relativity and states that inert mass is equal to gravitational mass. However, while many theories have been made, predicting a concordance (or not) between matter and antimatter, this principle has never been verified directly for antimatter. One way to do so is to observe the free fall of anti-matter atoms, to verify if antimatter's behavior is indeed the same than classical matter when subjected only to a gravitational field.

The experiment couples the ELENA experiment (CERN antiproton decelerator), and a linear accelerator that produces positrons to create positively charged antihydrogen atoms ($\overline{H}^+$, two positrons + one antiproton). The reason to use the charged form of antihydrogen is that ions are much easier to manipulate than neutral atoms, specifically for trapping them inside a Penning (or Paul) trap, and cool them down with lasers. Once cooled down to 10^-5 K, ions will have a typical speed of half a meter per second in the trap. Finally, a positron will be photo-detached from the $\overline{H}^+$ with the help of a laser, that will turn the ion into an electrically neutral $\overline{H}$ atom. Therefore, the atom will no longer be sensitive to the electromagnetic trap and will only experience the gravity. It will leave the trap, and fall 20 cm below into the detecting device in approximately 200 ms.

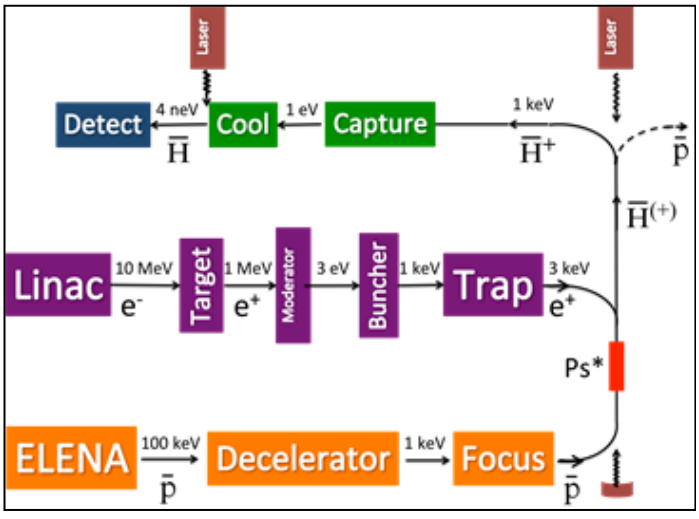

Figure 0: Schematic of the experiment GBAR, taken from https://gbar.web.cern.ch/GBAR/public/fr/design_fr.html

---

(1) In fact it has even been reassured in 2016 with the first direct detection of gravitational waves.

In the framework of the different techniques used for cooling down and manipulate trapped ions, the Doppler cooling allows single ions, small chains and even large ion ensembles containing 10^6 ions to be cooled down to a few mK. However, this technique is only available for certain atomic species or laser-cooled particles, because the corresponding atomic transition that would be used to cool down has no existing laser light source sufficiently powerful in that range of wavelength. Hydrogen atoms are part of that group, as the required laser technology is currently unavailable.

A method called sympathetic cooling was found to overcome that limitation, by using an ensemble composed of different species, one addressed by an accessible wavelength while the other is not. The sensitive one is directly cooled down, while the insensitive ion in the chain is cooled down by coulomb interaction with the neighboring ions. Until now, this technique has proven to be working for ions with comparable masses, up to a ratio of 3:1. The mass ratio of the atoms that will be used in the GBAR experience is 9:1 (beryllium and $\overline{\mathrm{H}}$). Questions are still open about the efficiency, the kinetics and the capture-range of sympathetic cooling in this unexplored regime.

In order to demonstrate experimentally the feasibility of this technique with mass ratio this large, the *Matériaux et Phénomènes Quantiques* (MPQ) and the *Laboratoire Kastler Brossel* (LKB) laboratories joined their equipments and efforts to investigate this issue.

The MPQ laboratory has the equipment and a decade experience with the trapping of Sr^+ ions, while the LKB has it for Be. The Sr^+/Be^+ ion pair has been chosen for experimentation because of its 9.8 mass ratio that is close to the one that will be used in GBAR, making this pair a very good candidate for this study.

The study of sympathetic cooling in the Doppler regime will be the first step, followed by the study of sympathetic cooling in the sideband regime, that will reach the lower temperatures needed by the CERN experiment.

Presentation of the laboratory and of the team

The MPQ laboratory of Paris Diderot University is a multidisciplinary research laboratory that studies quantum phenomena down to atomic scale, at the frontier with engineering and chemistry. This internship was done in the Quantum Information Technologies (QITE) group within the Trapped Ions team, which is specialized in the laser cooling of trapped ions confined in electromagnetic traps.

The team has designed and fabricated different trapping devices from a macroscopic Paul trap to a microscopic one on chip. The miniaturization experiments performed in the team participate to the effort of demonstrating building-blocks for quantum computing [1]. Indeed, laser cooled trapped ions are among the best candidates to realize quantum computers, notably thanks to easy quantum manipulation with lasers and long quantum coherence times [2].

Presentation of the internship subject: state of the art

As explained in the introduction, sympathetic cooling is a process in which laser-cooled particles of one species cool particles of another species. The effectiveness of it depends on the masses and charges ratios of the particles used. It has been reported for the first time by C. Myatt et al. in 1997. In the team, sympathetic cooling has been successfully done over the years with $^{88}Sr^+$ and its isotopes $^{87}Sr^+$, $^{86}Sr^+$ and $^{84}Sr^+$, although Sr and its isotopes have a mass ratio close to 1. The sympathetic cooling regime investigated with this project is quite different as the mass ratio of $\overline{H}^+$ and $^9Be^+$ is 9.8.

In the LKB, partner of this experiment, $^9Be^+$ ions are laser-cooled in order to sympathetically cool the H_2^+ molecule.

(1) M. D. Barrett, B. DeMarco, T. Schaetz, V. Meyer, D. Leibfried, J. Britton, J. Chiaverini, W. M. Itano, B. Jelenkovi´c, J. D. Jost, C. Langer, T. Rosenband & D. J. Wineland. *Sympathetic cooling of $^9Be^+$ and $^{24}Mg^+$ for quantum logic.* Phys. Rev. A, vol. 68, Oct 2003.

(2) Jonathan P. Home, David Hanneke, John D. Jost, Jason M. Amini, Dietrich Leibfried & David J. Wineland. *Complete Methods Set for Scalable Ion Trap Quantum Information Processing.* Science, vol. 325, no. 5945, 2009.

In articles **(1)** and **(2)**, the team report sympathetic cooling of $^9Be^+$ and $^{24}Mg^+$, as refrigerant, meaning that the $^{24}Mg^+$ was previously cooled before being sympathetically cooled by $^9Be^+$ (and vice versa).

(3) Xin Tong, Alexander H. Winney, and Stefan Willitsch, *Sympathetic Cooling of Molecular Ions in Selected Rotational and Vibrational States Produced by Threshold Photoionization.* Phys. Rev. Lett. 105, 143001 – Published 27 September 2010

In article **(3)**, authors report sympathetic cooling of N^{2+} Molecular Ions (28 a.m.u.) through $^{40}Ca^+$ laser cooling.

(4) E. R. Hudson (2016)3:8, *Sympathetic cooling of molecular ions with ultracold atoms.* EPJ Techniques and Instrumentation.

Article **(4)** reviews the progress of sympathetic cooling of molecular ions with ultra cold gases in the past years, with predictions of boundaries on mass ratios for the ions used that effectively allow sympathetic cooling to work. Cooling rates prediction are also given for a given parameter of trapping.

Chapter 1: Introduction to ions trapping and cooling

In this chapter, I will give a short (and mostly qualitative) overview of the Ion trapping and cooling.
Ion traps are devices that allows the confinement of charged particles in a given region of space, over a long period of time. They have been used widely in many different domains from mass spectrometry or metrology to quantum information.

It has been demonstrated that there is no static electric field that has a minimum for the electric potential, such that a charged particle could be trapped (Earnshaw's theorem in 1842). In order to overcome this issue, two different solutions have been found in the middle of the 20th century. The first one is called the Penning trap and uses a combination of electric and magnetic static fields to confine charged particles, while the other one is called Paul trap and uses static and time-dependent electric fields. We are interested in a particular case of the last one: the linear Paul trap.

1.1 The linear Paul trap

The linear Paul trap is made of two pairs of rod shaped electrodes and two sides electrodes called end-caps. A schematic of the device is drawn in **Figure 1.1**. The two pairs have a radio-frequency voltage applied that confines radially (x,y plane) forming therefore a quadrupole with potential:

$$\varphi(x,y,t) = \frac{V_{RF}\ (x^2 - y^2)\ \cos(\omega_{RF}\ t)}{r_0^2} \tag{1.1}$$

V_{RF} being the amplitude, ω_{RF} the oscillating pulsation potential, and r_0 is the distance separating the trap center and one electrode. The end-caps have static positive voltage applied to ensure axial confinement along z:

$$\varphi_{stat}(x,y,z) = \frac{V_{EC}\ (2z^2 - x^2 - y^2)}{2z_0^2} \tag{1.2}$$

where z_0 is half the characteristic length of the trap.

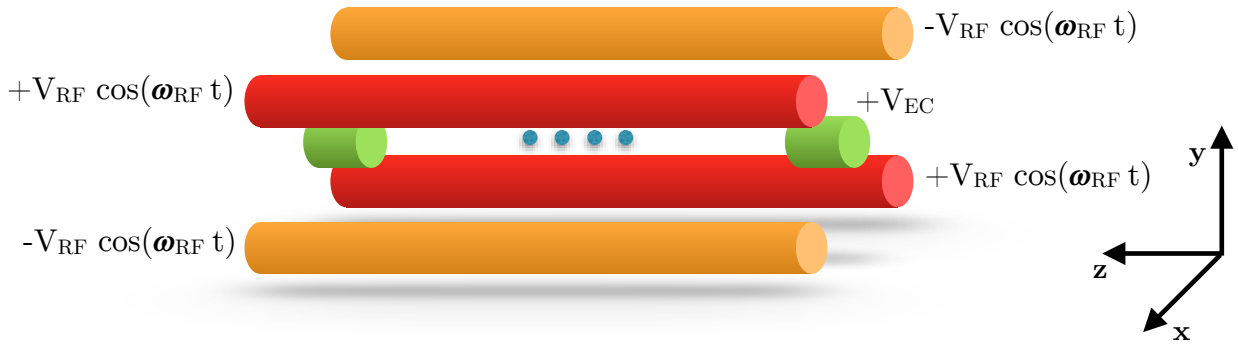

Figure 1.1: Schematic of a linear Paul trap. Reds and oranges rods have radio frequencies voltages applied (called RF rods later on), while greens ones have a static positive voltage applied (called end-caps later on). The blue dots represent four charged particles trapped in the center of the trap, where the RF field is supposed to be equal to zero.

1.2 Ion motion

The electric potential of equation (1.1) has a saddle shape, as depicted in **Figure 1.2**. For a positive ion in the center of the saddle, at the same given time t of the figure, the potential is confining along the axis x in the (x,y) plane, while it is repulses the charged particle away along the axis y. If we add $\boldsymbol{\pi}$ to the phase of the cosinus, the potential changes sign and is now repulsive along y and confining along x. If it is varying fast enough and in the right range of frequency(2), it can easily be pictured that such particle would be trapped. As previously said, the end-caps confine along the third axis with a static electric field.

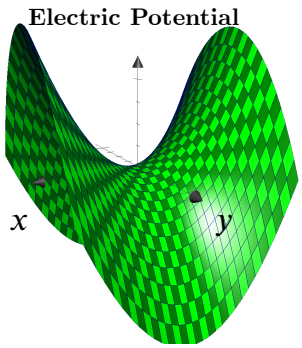

Figure 1.2: Shape of the electric potential at time t in the (x,y) plane corresponding to equation (1.1).

Ions motion in the (x,y) plane in a linear Paul traps is ruled by Matthieu's equations for which solutions are well known [3],[4],[5]. What needs to be kept in mind is that it exist a region of stability for ions in the center of the trap that depends on adjustable parameters ($\boldsymbol{\omega}_{\mathrm{RF}}$ and the amplitude of the RF for instance) and some that aren't (the mass of the ion or the physical dimensions of trap).

1.3 Ion creation

In order to obtain trapped ions, neutral Sr (or Be) has to be evaporated somewhere inside the vacuum chamber, then ionized near the center of the trap, because an ion generated outside the confinement zone cannot be trapped. The strontium evaporation is done by a Sr oven, which is composed of a tungsten filament that surrounds a Sr nugget. As a current from 1.3 up to 2 A flow in the filament, some Sr evaporates and spreads inside the chamber. The ionization is then usually obtained from an electron gun, or using photons (photoionization).

Initially, as the team didn't have the right laser source to photoionize the beryllium, it was thought that the Be ionization would be obtained using an electron gun. While for Sr ionization, the team was using a two-photon (of same frequency) absorption technique based on an infrared Titanium-Sapphire femtosecond laser tuned at 862 nm(3), and a non linear crystal for doubling the frequency to 431 nm as depicted in **Figure 1.3 a)**.

---

(2) The frequency needed depends on the mass of the particle we wish to trap. More details here [3],[4],[5].
(3) Titanium-Sapphire (*Spectra-Physics*, model Tsunami) pumped by a doubled Nd:YVO_4 @532 nm (*Spectra-Physics*, model Millennia Prime)

Sr^+ ions have been successfully obtain with the electron gun during setup of this experiment. However this method has inconveniences. First, it have the tendency to heat the whole chamber, therefore degrading the vacuum. Second, we have noticed that from one ionic crystal loading to the other, the center of the trap had the tendency to move in space. This was interpreted as electron accumulating on isolating pieces, perturbing the electric potential. Finally the ionizing rate was pretty low with this technique.

However during the setup of the experiment, we broke the filament of the electron gun by overestimating what it could handle. In order to avoid the replacement of this filament and all the consequences of it (going back to atmospheric pressure, opening the chamber in a controlled atmosphere of Ar etc...), it was thought that the Sr ionization could be done by a two-step photoionization technique using two different laser as depicted in **Figure 1.3 b)**, one of 405 nm and one of 461 nm. The Ti:Sapphire could now be tuned to emit at 940 nm to photoionize the beryllium atoms using two stages of frequency doubling, to obtain a continuous-wave 235 nm source, as in [10].

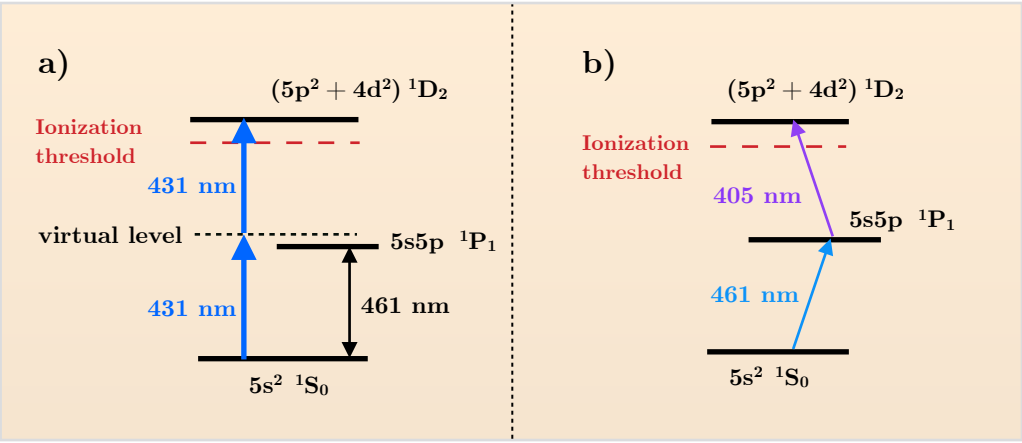

Figure 1.3: Electronic structure of neutral Sr for photoionization. $(5p^2 + 4d^2)\ ^1D_2$ level is self-ionizing. **a)** Two-photon absorption technique with two photons of same energy doubled from infrared femto-laser. **b)** Two-step ionization technique using two photons of different energies.

1.4 Doppler cooling of trapped ions

The Doppler cooling is a technique based on laser to cool down atoms or ions. The principle of working is the same for atoms and ions, except that due to the electric confinement in the case of trapped ions, only one direction of laser illumination is needed, provided that this direction has a component in each proper axes of the trap. Thus, I will focus on the Doppler cooling of trapped ions.

Let's consider first a two level ion at rest. When a photon is absorbed by an ion, the impulsion $\hbar \mathrm{k}$ of the photon is transmitted to the ion, and it gets in its excited state. The spontaneous emission being an isotropic process, ions are on average only subjected to a force directed according to the wave vector's direction of the laser, which is called radiation pressure force and is compensated by the restoring force induced by the trap. Now if the ion is moving with a velocity v on the laser axis, it will « see » the frequency of the laser shifted from the frequency seen at rest, due to Doppler effect.

By applying a small detuning $\Delta = \omega_{laser} - \omega_{res}$, to the pulsation ω_{laser} of our laser as it can be seen on **Figure 1.4 a)**, the ion will absorb more photons if it is moving towards the laser, such that a part of its kinetic energy will be brought to accomplish this transition, reducing therefore its velocity. Later, the spontaneous emission will reemit a photon of same energy in a random direction of space, that will also as previously said, produce a force that is null on average for large number of excitation-spontaneous emission cycle. Applying this cycle a lot of times will continuously reduce the velocity of ions interacting with the laser till the Doppler temperature limit define as:

$$T_{Doppler} = \frac{\hbar \gamma}{2 k_B} \simeq 1 \text{ mK} \tag{1.4}$$

with $\hbar$ being the reduced planck constant, γ the natural linewidth of the cooling transition and k_B the Boltzmann constant. In practice the temperature obtained at the end is a bit larger, because the RF field forced motion (micromotion) can result in a warm up of the ions.

However, even though in certain conditions the two-level atoms gives sufficient prediction for Strontium ions, it is more accurate to describe it as a three level atom as depicted in **Figure 1.4 b)**. Indeed, the deexcitation from the $P_{3/2}$ upper level can either bring back the ion in the fundamental level with a certain probability or in the metastable $D_{3/2}$ level, for which the down transition to the fundamental is forbidden. Thus, after a certain time if not re-pumped, all ions will remain in the metastable level and cooling no longer occurs. This is overcome by using a second laser, that will constantly bring back ions in the $P_{3/2}$ level.

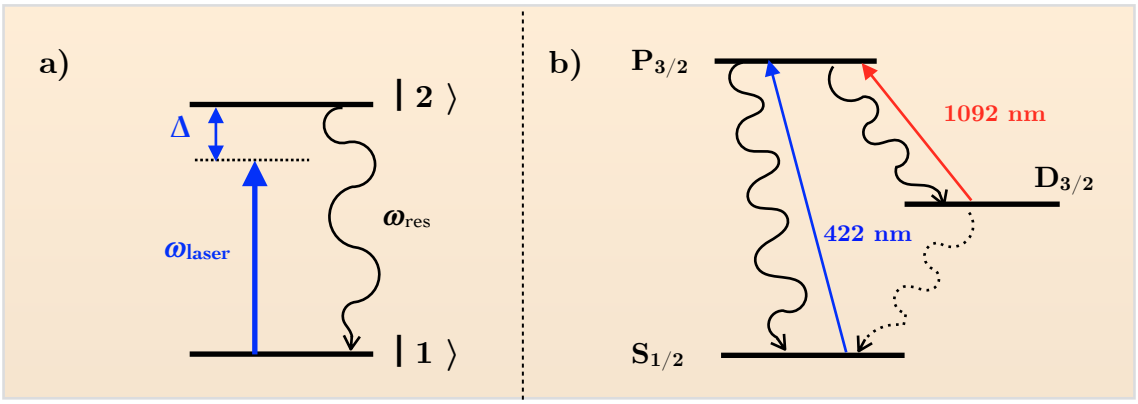

Figure 1.4: **a)** Two-level atomic system. ω_{laser} is the pulsation of the cooling laser detuned of Δ compared to the resonant transition pulsation ω_{res}. **b)** Energy level diagram used for Doppler cooling of $^{88}Sr^{+}$ ions. Blue line is the transition used for cooling. Red line is the re-pumping transition. Black lines are spontaneous deexcitation, while the black dotted line is not allowed.

Chapter 2: Presentation of the experiment

When I arrived in the team, the vacuum chamber had already been built and was undergoing turbo molecular pumping. Baking started soon after. During the baking period and after, I was in charge of the pressure monitoring and the survey of the chemical species present in the chamber, this until the lowest pressure has been reached (2E-10 mbar).

2.1 Experimental Setup

The setup of the experiment is depicted below in **Figure 2.1**. It is composed of a large chamber with a diameter ≃ 40 cm, with different viewports of different sizes, two for observations ((8) and a top one not depicted), while two others are made for the entrance of lasers and their alignment with the center of the trap ((2) and (5)). All parts inside the chamber has been previously cleaned before the assembling to avoid contamination. The final assembling is done in an argon atmosphere to prevent contamination.

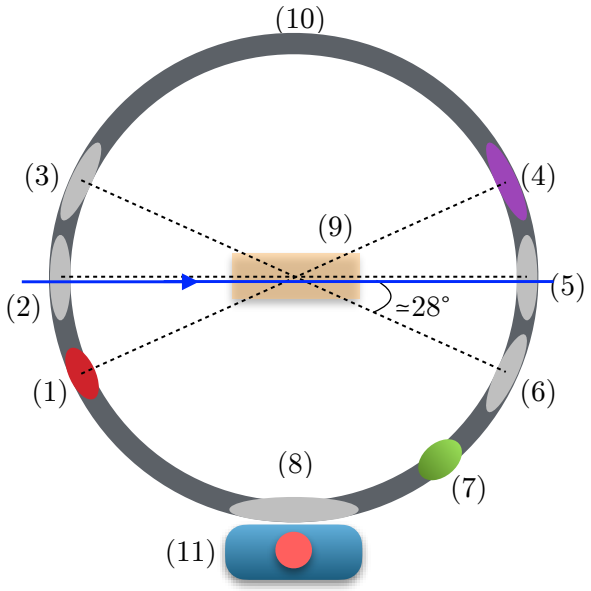

(1) Main Sr oven
(2) Laser entrance
(3) Ex-entrance of the femto laser
(4) Residual gaz analyser (RGA)
(5) Laser exit
(6) Viewport
(7) Pfeiffer vacuum gauge IKR 270
(8) Observation porthole
(9) Linear Paul trap
(10) Vacuum chamber
(11) Side Camera

Figure 2.1: Schematic top view of the vacuum chamber setup. Pumps, electron gun, Be ovens and the second Sr oven are not represented.

2.2 Vacuum techniques and monitoring

Among the different techniques that I used during the internship, the vacuum techniques has taken an important part. Indeed, experiments with ion traps require to be in ultra high vacuum to avoid any source of perturbation or heating from collision with the environment. In the best conditions, the pressure inside our vacuum chamber can go down to 2E-10 mbar.
Different pumping devices are necessary to reach this kind of pressure, because no single vacuum pump can reach ultra high vacuum from atmospheric pressure. The first step of pumping is realized through a primary pump that allows the chamber to reach 10^{-2} - 10^{-3} mbar. A turbo-molecular pump takes over to go down to 10^-7 mbar from the mbar pressure. At this time, it is required to bake the chamber up to 160°C for several days to outgas all kinds of chemicals, molecules or atoms that have been adsorbed by the surfaces inside the chamber during their previous life at atmospheric pressure.

To do so, a flexible heating band is enrolled around the vacuum chamber and tuned to slowly warm it, up to the desired baking temperature[4]. During the baking, the chamber is wrapped with aluminium to keep the heat. The ovens inside the chamber used to release the Sr and Be are also turned on to get rid of the impurities and possible contamination adsorbed during the assembling. A typical pressure plot[5] during outgassing of ovens can be found in **Figure 2.2.3**, note that among the different contaminants we outgas with the ovens, we also release the specific element these ovens are made to dispense, that is Be and Sr in our case. The quantity wasted is however totally negligible compared to the size of the nugget and it does not affect substantially the lifetime of the oven. This procedure of baking under turbo-molecular pumping allows to gain typically an order of magnitude in pressure (10^-8 mbar).

During the secondary pumping (P<10^-6 mbar), a residual gas analyzer (RGA) is used to monitor in quantity the different species inside the vacuum chamber [6]. It gives us great information about the quality of the vacuum and it is also a good help when a leak is suspected. A typical mass spectrum scan can be seen in **Figure 2.2.1**.

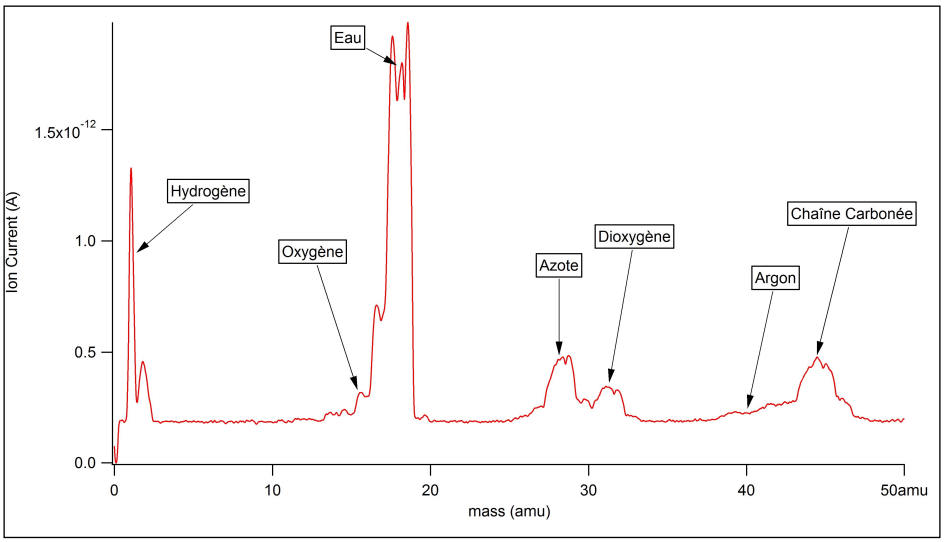

Figure 2.2.1: Ion current(A) in function of the mass (amu), a scan from 0 to 50 amu takes 100 sec (2sec/amu).

From the data of the RGA, we can track the variation of each species in function of time. A little program has been written with IGOR Pro to take care of the sorting of data and the plotting. At the end of each scan, the background is determined by averaging abscissa regions known to be empty in terms of species (at least in our case), and it is then subtracted. An integration method is then used to track the evolution of each species. It consist of preselecting each region surrounding a peak, typically when the ion current starts to get larger than the noise, and integrate it[7]. It is then plotted in function of time, as in **Figures 2.2.2**, **2.2.3**, **2.2.4**.

---

(4) Typically 1°C per minute as the portholes of the chamber are very sensitive to temperature changes.
(5) Measured with Pfeiffer vacuum gauge, model IKR 270, sensitive down to 5E-11 mbar.
(6) Model Pfeiffer vacuum PrismaPlus, it was once used to find a leak present in the system, with the help of an external helium source.
(7) It has been verified carefully that there was no noticeable peak derive or shift in function of time.

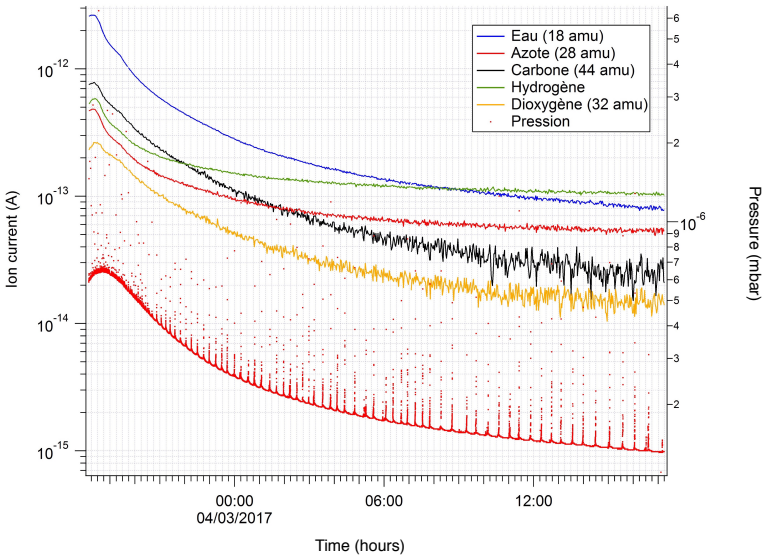

Figure 2.2.2: Tracking of pressure and the concentration of the different species detected inside the chamber by the RGA. One hour before the acquisition of data, the baking was launched for a few days @140°C, explaining the rise of pressure and the different species concentrations due to heating. It then starts to drop as the outgassed elements get pumped.

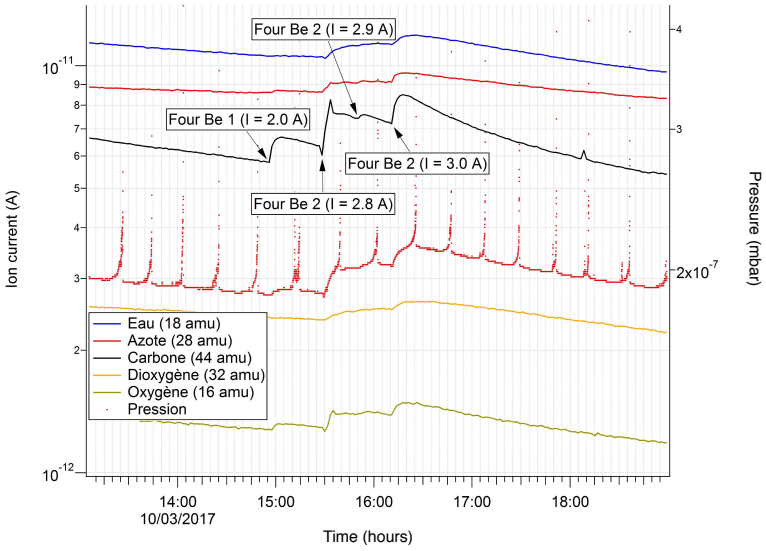

Figure 2.2.3: As a current flows inside ovens, outgassing occurs with a rise of temperature, pressure and concentration of tracked species.

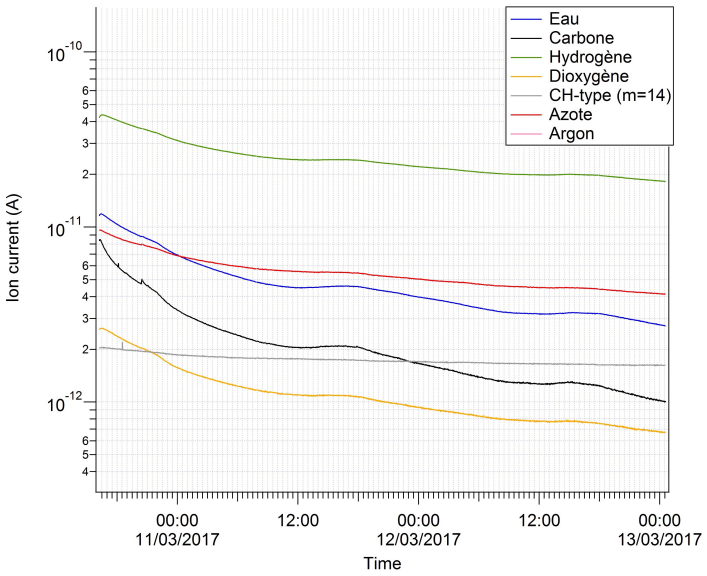

Figure 2.2.4: Concentrations of species decreasing over time during baking. Water (blue) and carbon (black) are well pumped, while Hydrogen (green) or nitrogen (red) are less pumped.

An ionic pump is finally used allowing the pressure to tickle the 10^-11 mbar in the best conditions. It is supported by a titanium sublimation pump that is basically a titanium wire in which a 38 amps current is applied. Doing so, the titanium filament reaches its sublimation temperature, spreading some clean titanium on the chamber's walls. Species colliding the walls will be adsorbed because of the high reactivity of clean titanium, therefore reducing the pressure of the chamber. At the same time, it also regenerates the ionic pump titanium's cathode. This process is typically applied twice a day. Note that inert gas as argon are badly pumped using the ionic pump.

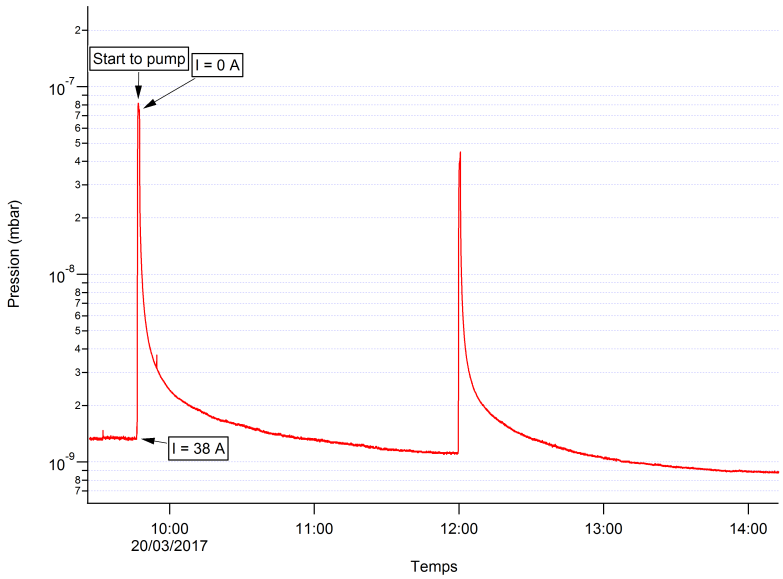

Figure 2.2.5: Pressure in function of time. Two 1min long titanium sublimations, spaced by approximately 2 hours, allowing to reduce the pressure in the chamber.

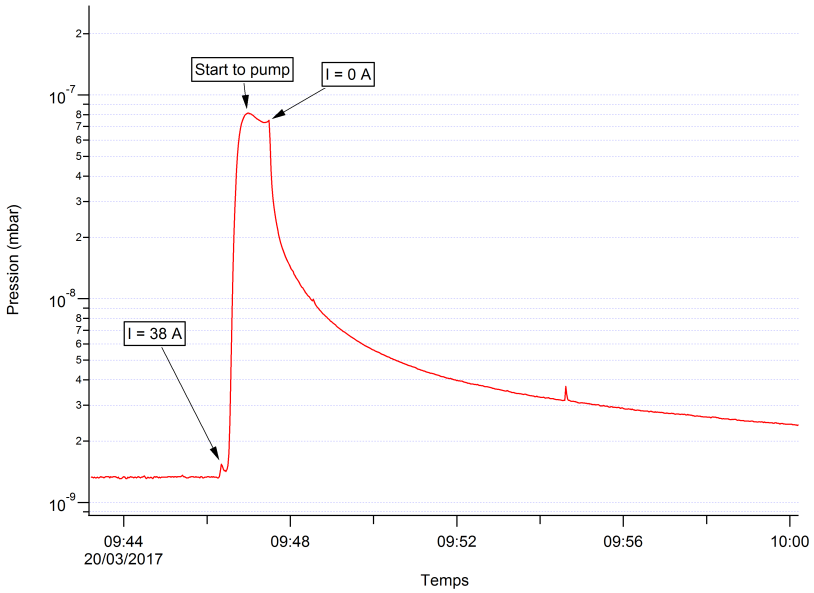

Figure 2.2.6: Zoom (in time) on the 1st sublimation from **Figure 2.2.5**. As the 38 amps current is applied on the titanium filament for one minute, temperature rises quickly and titanium is expelled of the filament to the wall of the chamber. Pressure increase quickly due to the titanium being released, then starts to drop (while current is still applied) because the wall of the chamber starts to pump elements by adsorption. The convenient moment to cut off the current is when the pressure starts to go up again, due to the fact that we heat more than we pump.

2.3 Optical bench

In this part I will present in detail the photoionization's optical bench as I have participate for its setup, then shortly present our 422nm and infrared sources coming from the micro-trap experiment and how they are locked, as they were mostly already set up when I arrived.

Photoionization's optical setup next to the vacuum chamber is depicted in **Figure 2.3** below. We use a 461 nm external cavity diode laser (ECDL) to address the transition of **Figure 1.3 b)** (p10). It is powered with a regulated power supply, with a module that regulates the temperature of the Peltier below the diode. This diode is not locked and has a typical (direct) output power of 10 mW. Until now, the tuning procedure is done by roughly playing between the diode current and the PZT's voltage that moves the diffraction grating, until the wavelength meter display the resonating transition's pulsation of 650508 GHz. Then a more accurate tuning is done by turning on the Sr oven to 2A, watch the live CCD camera's video stream on a computer display and look for the fluorescence of neutral Sr, while carefully adjusting the PZT's voltage to maximize it once found (see **Figure 3.1**).

We use a free running 405 nm GaN laser diode to address the the transition of **Figure 1.3 b)**. It is also powered with a regulated power supply, with a PID controlled Peltier element. The wavelength emitted was roughly adjusted by tuning the temperature set point with the help of a spectrometer as detailed later on in **Chapter 3**. This diode isn't locked and has a typical (direct) output power of 3 mW.

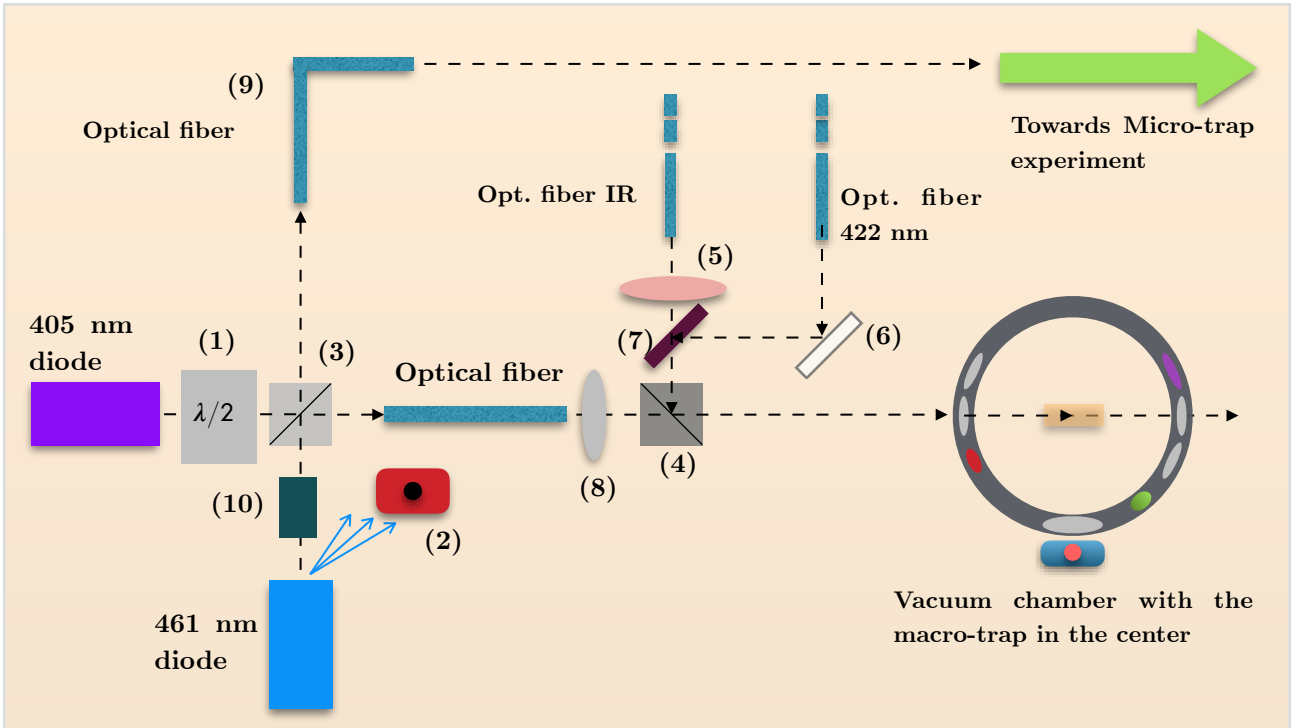

Figure 2.3: Optical bench of the macro-trap experiment. **(1)** The $\lambda/2$ waveplate is fixed in a rotary mount to modify the power of the 405 nm laser diode impinging on the trap, without having to change the current. **(2)** A wavelength meter model Wavemaster from *Coherent,* is put near the exit of the 461 nm laser diode to pick up some diffusion, GHz resolution. **(3)** Beamsplitter. **(4)** Polarizing beamsplitter. **(5)** Lens for focusing the infrared laser in the center of the trap. **(6)** Mirror **(7)** Dichroic infrared mirror **(8)** Lens for focusing the two blues in the center of the trap. **(9)** Optical fibers are used for dispatching beams, but also for filtering modes as it is ideal to have a TEM_{00} for reducing diffusion in the center of the trap. **(10)** Optical isolator.

In order to address the cooling and re-pumping transition described in **Figure 1.4 b)**, we need tunable single-modes laser sources stable in time.

The cooling transition of $^{88}Sr^{+}$ ions is addressed by an ECDL tunable around 422nm, made by *Toptica Photonics* (model DL100), with 10mW of power. It is stabilized in temperature thanks to a water-cooling system and a Peltier device. The re-pumping transition is addressed by an infrared fibered laser made by Koheras (model Adjustik Y10), tunable around 1092 nm with 10 mW of power.

Due to the fact that the frequencies of our lasers drift in time, and as a precision of a fraction of $\gamma/2\pi$ is required (typically 2 MHz) in order to address transitions efficiently, we need to be able to lock all frequencies. By chance, the cooling transition of $^{88}Sr^{+}$ that we use is almost in exact coincidence with the transitions $5s^2\ S_{1/2}(F=2)\ 6p^2\ P_{1/2}(F'=2)$ and $5s^2\ S_{1/2}(F=2)\ 6p^2\ P_{1/2}(F'=3)$ of ^{85}Rb ($\nu_{Sr^{+}}$ - ν_{Rb} is respectively 440 and 567 MHz). Thus, the cooling laser is locked using a rubidium vapor cell heated to 140°C, to form a saturated absorption setup.

The beam sent to the trap is frequency-shifted by a double pass in an acousto-optic modulator (AOM) driven around 200MHz, therefore shifting the frequency of the beam by 2 x 200MHz, 40 MHz away from the resonance of the cooling transition. The precise detuning Δ used for Doppler cooling (**Figure 1.4 a)**), is set choosing the driving frequency of the AOM.

At last, the re-pumping laser is locked on a ring cavity referenced to the 422 nm diode. The length of the cavity is tuned using a PZT fixed behind one of the mirror of the ring cavity.

More recently, Vincent Tugayé currently doing his PhD thesis in the group, has improved the addressing by also taking into account shifts due to variations of the temperature, pressure and humidity of the experiment room.

Chapter 3: Results

3.1 Ions observation and determination of a crystal density

$^{88}Sr^{+}$ ions are observed through fluorescence as they spontaneously deexcitate from state $P_{1/2}$ to $S_{1/2}$, during Doppler cooling as seen on **Figure 1.4 b)**. It is relatively easy to observe as the absorption - emission cycle is very frequent (order of MHz). It is observed in our experiment through a viewport with a CCD camera. When the temperature of the ion cloud is sufficiently low, a phase transition occurs toward an ordered phase called Coulomb crystal. We have been able to load and observe a single fluorescing ion up to large crystals composed of several million of ions. With intermediate number of ions lets say 50, the shape of the crystal can be manipulated by changing the electric field. Doing so, ellipsoids, spheres or string crystal can be created.

In figure **Figure 3.1.1**, I have loaded a large crystal with an ellipsoid shape. The centered darker region of the crystal has a cylindrical shape in 3D. It is composed by $^{87}Sr^{+}$, $^{86}Sr^{+}$ and $^{84}Sr^{+}$ that are sympathetically cooled by the thick surrounding envelope of $^{88}Sr^{+}$, itself cooled by Doppler cooling. Therefore, what is observed is a fluorescing ellipsoid with a « hole » in the center (see **Figure 3.1.2 b)**).

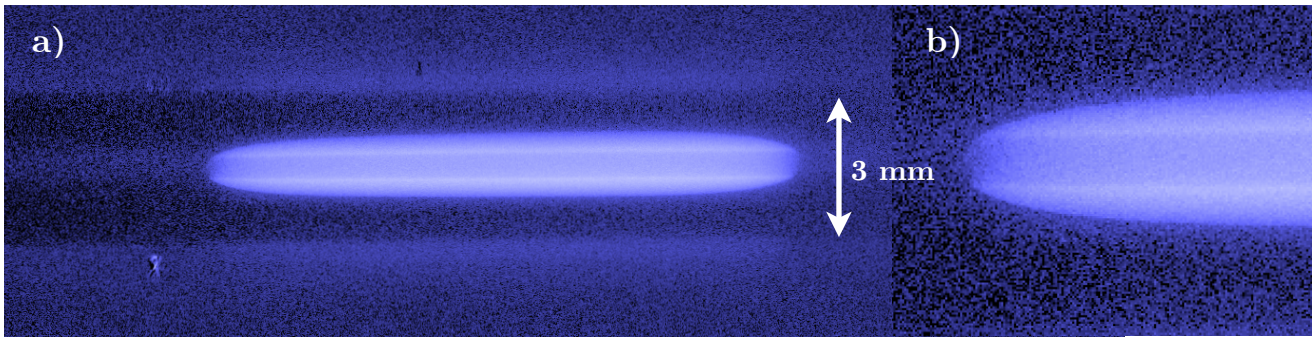

Figure 3.1.1: **a)** Picture in false color of a large ionic crystal loaded in 1 min of photoionization. The top and bottom region are the electrodes, the fluorescence is reflected on it. The bright line on the left (and a bit less on the right) on the same axe of the crystal, is the fluorescence of the neutral Sr, as the 461 nm laser shutter has been left on. **b)** Same crystal zoomed on the left edge, segregation between different Sr^{+} isotope is visible.

A good estimation of this crystal density $\boldsymbol{\rho}_0$ can be computed considering a crystal at zero temperature, using the following equation:

$$\boldsymbol{\rho}_0 = \frac{\boldsymbol{\varepsilon}_0 \, {V_{RF}}^2}{m \, {r_0}^4 \, {\boldsymbol{\omega}_{RF}}^2} \qquad \textbf{(3.1.1)}$$

where $\boldsymbol{\varepsilon}_0$ is the vacuum permittivity, V_{RF} is the RF voltage amplitude, m the mass of the Sr^{+} ion, r_0 is the radius between the center of the trap and an electrode and $\boldsymbol{\omega}_{RF}$ is the pulsation of the RF.

In order to determine with precision the size of this crystal, I used a program written by the team in IGOR Pro, that cut slices of an image over a certain range in X (or Y), average the intensity received by the pixels in that range, and gives in output this average pixel intensity along Y (resp. X). **Figure 3.1.2** is obtained by doing so[8].

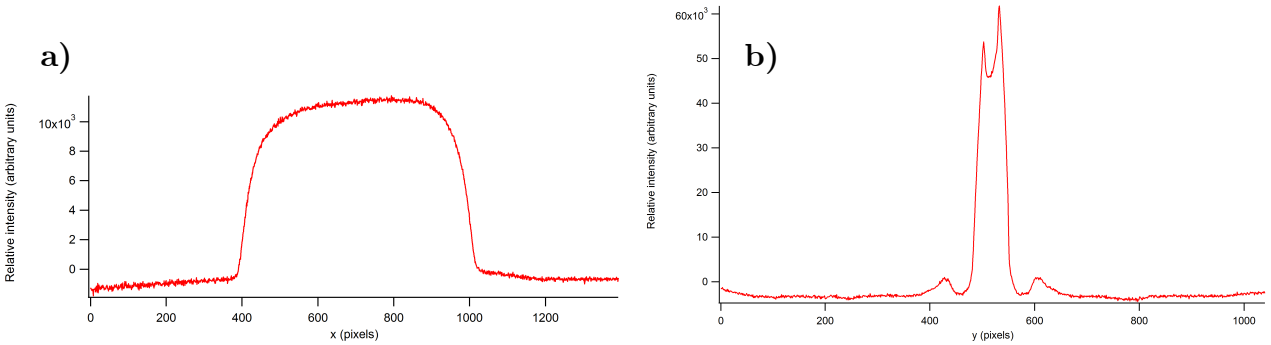

Figure 3.1.2: Plots of relative intensity received by a slice of pixels in an acquired image in function of the pixel's position. It greatly helps for determining the size of the crystal in pixel. **a)** Slice along Y of an image captured by the camera. **b)** Same than a) but along X.

The little side hills visible on **Figure 3.1.2 b)** come from the reflection of the fluorescence on the electrodes, while the main peak has a hole in the middle due to non fluorescing sympathetically cooled Sr^{+} isotopes in the center of the ellipsoid.

As we know that the distance between two electrodes is 3 mm, we can convert pixel lengths into a lengths in I.S. units. With good approximations, we suppose the depth of the crystal (which is not accessible with this image alone) is the equal to the height. The volume of an ellipsoid is define as:

$$V = \frac{\pi \times x \times y \times z}{6} \qquad \textbf{(3.1.2)}$$

We obtain a 1.4 mm diameter, a length of 19.3 mm, a density of 3.27×10^{14} m^{-3}, thus approximately 6.48 million ions in this crystal. Furthermore, we can estimate an average photoionization rate for this loading by dividing the number of ions over the time spent to load, which is 60 seconds.

This gives 1.08×10^{5} ions/sec, which is greater than the previous photoionization rates reached by the team [6].

(8) This procedure was used to measure all cristals sizes in the following.

3.2 Characterization of the 405 nm diode and of the 5s5p $^1P_1 \longrightarrow 5p^2\ ^1D_2$ transition

In order to have a better insight on the dependance of the 405 nm diode on the photoionization rate, it is important to characterize it. I have started by measuring the output power (measured directly outside the diode) as a function of the diode current for a given set point of temperature, (see **Figure 3.2.1**). Later on I probed the temperature dependence of the emitted wavelength, by keeping the current constant (inset of **Figure 3.2.1**).

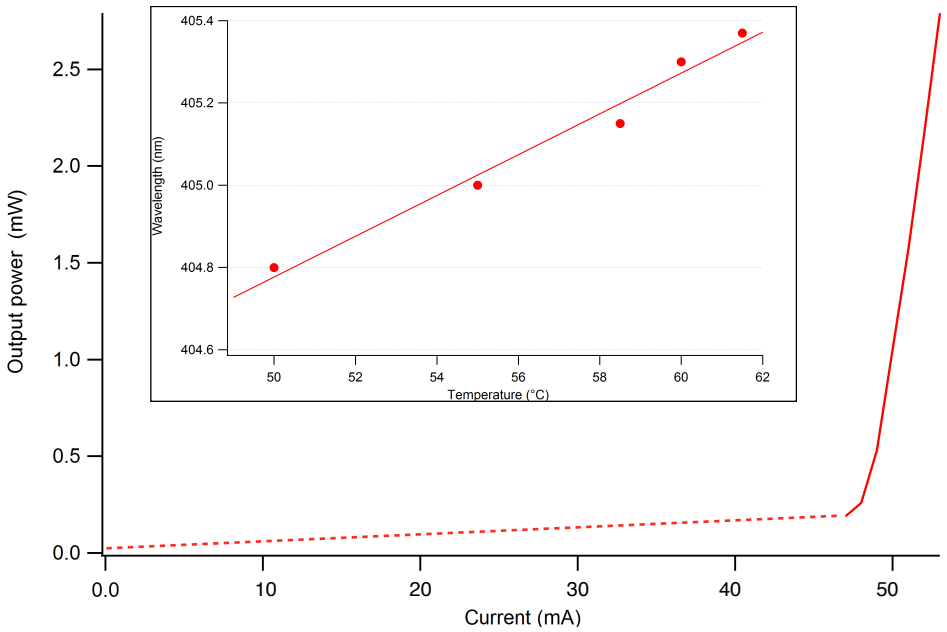

Figure 3.2.1: Output power vs current. Lasing threshold at ≈48 mA. Dotted line was not measured but added for visibility. Inset: Wavelength corresponding to the peak intensity emitted by the diode as a function of the temperature. Peak wavelength measured with a *BWTek* CCD array spectrometer, model BRC112E.

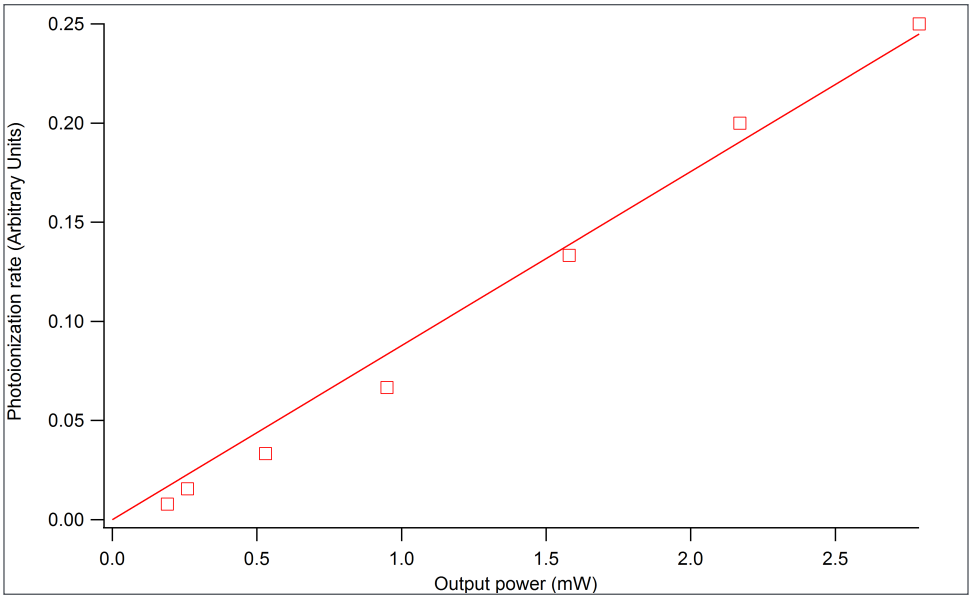

Figure 3.2.2: Photoionization rate (prop) in function of Output power. Output power here was measured at the laser exit.

I have then measured the time needed to load a Coulomb crystal of a given size as a function of the output power of the 405 nm diode in **Figure 3.2.2**, and made sure the photoionization rate was linear by plotting a relative photoionization rate obtained by taking the inverse of the loading times.

According to [7],[8] and [9], the peak wavelength corresponding to the 5s5p $^1P_1 \rightarrow 5p^2\ ^1D_2$ Sr transition is 405.2 nm. According to my measurements in **Figure 3.2.1**, if we want to optimize this transition we should tune the temperature set point of this diode around 59°C. I have tried to find experimentally this corresponding wavelength transition by measuring the photoionization rate as a in function of the wavelength (by varying the temperature set point between each measurement). This, for a given loading time of 30 seconds, while keeping constant the applied current and the power output at the exit of the trap. It was not an easy task as the number of parameters to keep constant was very large. Indeed, the output power of all laser had to be the same during all measurements (therefore verified after each loading). While the re-pumping and the cooling laser are stable for several hours once locked, the 461 nm laser is stable in power but the frequency can shift of a GHz over an hour. A spectrum had to be acquired with the spectrometer during each loading. Image of each crystal saved and kept aside for data analysis as previously detailed. The crystal acquisition procedure was the following: A small seed crystal of a given size was first created by turning on the 405nm diode shutter for less than a second then turned off. This was done in order to observe the crystal growth in real time, as the loading dynamic may depend on the temperature of the ions (the fact that it is crystalized or not). Indeed, our photoionization was so efficient that for the two largest crystal obtain in **Figure 3.2.3**, the seed was breaking almost instantaneously, and crystallization was occurring again few seconds later, in the middle of the loading. Therefore a higher uncertainty is expected for these two points. Two loading measures were done for each wavelength, and the mean crystal volume of the two is plotted in **Figure 3.2.3**. Error bars defined as the difference of the two crystal volume, divided by 2 (Seed melting not taking into account in the presented error bars, but it should be kept in mind). We obtain a peak at 405.3 nm, close to what has been reported.

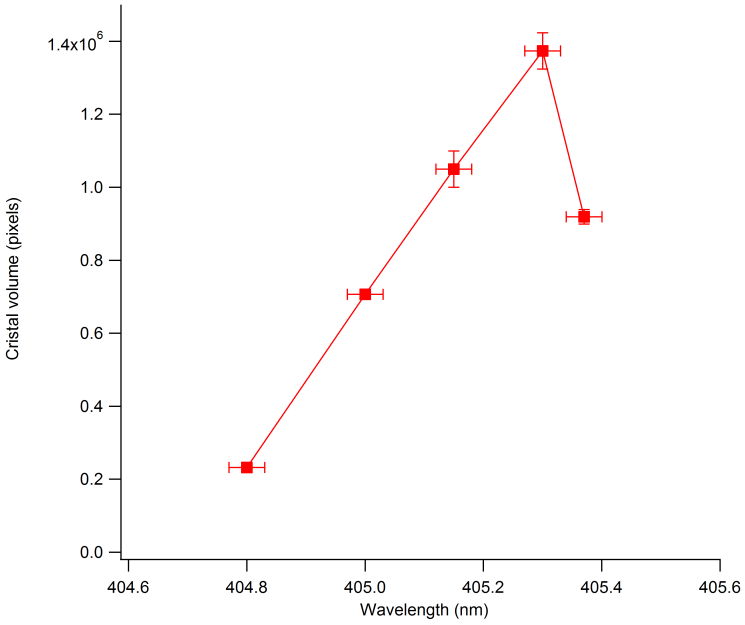

I report the following parameter used for the electrodes: V_{EC} = 48V, V_{RF} = 297V, $\omega_{RF} = 2\pi \times 7.62$ MHz.
The output power of laser kept constant, and measured after the trap:
$P_{405} = 20\ \mu W$, $P_{422} = 220\ \mu W$, $P_{461} = 320\ \mu W$ and $P_{1092} = 420\ \mu W$.

Figure 3.2.3: Cristal volume in pixels, obtain for a given time of loading in function of the wavelength of the 405 nm diode. The peak is located at 405.3nm.

Conclusion and prospects

The reader may have noticed that there is no deep examination of the sympathetic cooling in this report. The reason for this is that the experiment was at the dawn of the implementation when I arrived. Therefore most of my internship work was concerning the setup of the experiment including the vacuum techniques, the ionization, the trapping and cooling of Sr^+ ions in a linear Paul trap.

However, a vacuum of good quality, lower than the one aimed has been successfully reached. A new technique of photoionization of Sr^+ using two laser has been setup in the group, and is accessible to both trapping experiment. Moreover the photoionization rate is now improved by at least on order of magnitude. Finally trapping and cooling of Sr^+ ions has been successfully obtain in relatively short times.

At the time I am writing these lines, the ionization optical bench of Be^+ has been set up, but hasn't been tested in the right conditions. Indeed, our only chance to observe the success of the photoionization of Be^+, is to observe the sympathetic cooling of Be^+ ion(s) by Doppler cooling of Sr^+ crystals, as we currently do not own the right laser to perform a Doppler cooling of Be^+. We spent some time trying to sympathetically cool Be^+ without optimizing the stability region for both Be^+ and Sr^+ (that depends on the voltage and frequency of the RF). But of course It would have been too easy, and the negative outcome was predictable as different trapping parameters than the one used are required for trapping Be^+. We are currently trying out to find a stable region for both Be^+, Sr^+ and therefore, as I am finishing my internship, the feasibility of sympathetic cooling of Be^+ ion(s) in a Sr^+ crystal is still ahead of us, at least for the moment.

Bibliography

[1] R. Blatt, D. Wineland, *Entangled states of trapped atomic ions.* Nature 453, 1008–1015 (2008).

[2] T. P. Harty, D. T. C. Allcock, C. J. Ballance, L. Guidoni, H. A. Janacek, N. M. Linke, D. N. Stacey, D. M. Lucas, *High-fidelity preparation, gates, memory, and readout of a trapped-ion quantum bit.* Phys. Rev. Lett. 113, 220501 (2014)

[3] S. Rémoville. *Vers une mémoire quantique dans des ions piégés.* PhD thesis, Université Paris Diderot - Paris 7, 2009.

[4] R. Dubessy. *Réalisation, étude et exploitation d'ensembles d'ions refroidis par laser stockés dans des pièges micro-fabriqués pour l'information quantique.* Université Paris-Diderot - Paris VII, 2010.

[5] B. Szymanski. *Piégeage et refroidissement d'ions strontium dans des pièges micro-fabriqués.* PhD thesis, Université Paris Diderot - Paris 7, 2013.

[6] B. Dubost. *Light-matter interaction with atomic ensembles.* PhD thesis, Université Paris Diderot - Paris 7, Universitat Politècnica de Catalunya, 2012

[7] Sami-ul-Haq, S. Mahmood, N. Amin, Y. Jamil, R. Ali and M. A. Baig, *Measurements of photoionization cross sections from the 5s5p $^1P_1$ and 5s6s $^1S_0$ excited states of strontium.* J. Phys. B: At. Mol. Opt. Phys. 39 (2006).

[8] K. Vant∗, J. Chiaverini, W. Lybarger, and D. J. Berkeland, *Photoionization of strontium for trapped-ion quantum information processing.* arXiv, 7 July 2006.

[9] M.A. Baig , M. Yaseen, Raheel Ali, Ali Nadeem, S.A. Bhatti, *Near-threshold photoionization spectra of strontium.* Chemical Physics Letters, Nov 1998.

[10] Hsiang-Yu Lo et al. *All-solid-state continuous-wave laser systems for ionization, cooling and quantum state manipulation of beryllium ions.* Appl. Phys. B, 114:17-25 (2014)